

Multiwavelength Observations of Supersonic Plasma Blob Triggered by Reconnection Generated Velocity Pulse in AR10808

A.K. Srivastava^{1,2} · R. Erdélyi² ·
K. Murawski³ · Pankaj Kumar⁴ ·

© Springer ●●●

Abstract Using multi-wavelength observations of Solar and Heliospheric Observatory (SoHO)/Michelson Doppler Imager (MDI), Transition Region and Coronal Explorer (TRACE) 171 Å, and H α from Culgoora Solar Observatory at Narrabri, Australia, we present a unique observational signature of a propagating supersonic plasma blob before an M6.2 class solar flare in AR10808 on 9th September 2005. The blob was observed between 05:27 UT to 05:32 UT with almost a constant shape for the first 2-3 minutes, and thereafter it quickly vanished in the corona. The observed lower bound speed of the blob is estimated as ~ 215 km s⁻¹ in its dynamical phase. The evidence of the blob with almost similar shape and velocity concurrent in H α and TRACE 171 Å supports its formation by multi-temperature plasma. The energy release by a recurrent 3-D reconnection process via the separator dome below the magnetic null point, between the emerging flux and pre-existing field lines in the lower solar atmosphere, is found to be the driver of a radial velocity pulse outwards that accelerates this plasma blob in the solar atmosphere. In support of identification of the possible driver of the observed eruption, we solve the two-dimensional ideal magnetohydrodynamic equations numerically to simulate the observed supersonic plasma blob. The numerical modelling closely match the observed velocity, evolution of multi-temperature plasma, and quick vanishing of the blob found in the observations. Under typical coronal conditions, such blobs may also carry an energy flux of 7.0×10^6 ergs cm⁻² s⁻¹ to re-balance the coronal losses above active regions.

Keywords: Flares, Flux tubes, Magnetic fields, Corona

^{1,2} Aryabhata Research Institute of Observational Sciences (ARIES), Nainital, India. email: aks@aries.res.in

²Solar Physics and Space Plasma Research Centre (SP²RC), School of Mathematics and Statistics, The University of Sheffield, Sheffield, U.K.

³Group of Astrophysics, UMCS, ul. Radziszewskiego 10, 20-031 Lublin, Poland.

⁴Korea Astronomy and Space Science Institute (KASI), Daejeon, 305-348, Republic of Korea.

1. Introduction

Large-scale solar transient phenomena (solar flares and CMEs) are examples of the magnetic dynamical and highly energetic processes of the Sun during which the energy stored in the sheared and twisted magnetic structures is rapidly released in the form of particle acceleration, plasma heating and bulk mass motion within from a few minutes to a few tens of minutes timescales. However, the exact mechanism of the initiation and triggering of solar flares and coronal mass ejections (CMEs) since the discovery of the first flare by R.C. Carrington on 1st September, 1859 is still not yet known in full details. It is well explored that the flares may occur near the magnetic null points, and current sheets are formed by instability near the neutral point where field lines exhibit a magnetic reconnection process. Reconnection can be an efficient mechanism of converting magnetic energy to thermal and bulk kinetic energies and to accelerate particles (Benz, 2008). The novel observational signature of 3-D X-type loop-loop interaction and the flare triggering due to reconnection in an active magnetic complex has recently been reported by Kumar *et al.* (2010). It is also found that the instabilities (kink, magnetic Kelvin-Helmholtz, coalescence, etc.) can also be one of the favourable mechanisms to trigger solar flares with or without CMEs (Liu, Alexander, and Gilbert, 2007; Srivastava *et al.*, 2010; Kumar *et al.*, 2010; Foullon *et al.*, 2011; Botha, Arber, and Srivastava, 2012). In conclusion, appropriately correlated theoretical and observational studies of these phenomena are still needed to be explored to understand the complex dynamical processes at the Sun.

In spite of a number of attempts to analyse the energy build-up and energy release processes associated with the eruptive phenomena, the recent trend has also been evolved to study the responses of solar eruptions on the plasma dynamics and the generation of periodic (quasi-periodic) oscillation patterns during these energetic events. These natural responses to the highly energetic solar eruptive phenomena are very useful in diagnosing and constraining the local plasma conditions of the solar atmosphere. The high-speed plasmoids associated with CME eruptions (Sheeley and Wang, 2002; Manoharan and Kundu, 2003; Lin *et al.*, 2005; Riley *et al.*, 2007; Milligan *et al.*, 2010), chromospheric evaporation (Veronig *et al.*, 2010), very high-speed outflows (Wang *et al.*, 2006), downflows and plasma condensations (Yokoyama *et al.*, 2001) in the course of flaring activities have been extensively studied. The secondary plasmoids can also be evolved in the eruptive region due to the plasmoid instability in a sufficiently long and thin current layer (Loureiro, Schekochihin, and Cowley, 2007). Therefore, they are associated with reconnection, however, not directly with CMEs. The ejecta can only generate the favorable conditions for plasmoid instability by formation of elongated and stretched current sheet in the active region. Periodic and quasi-periodic MHD oscillations have also been observed and studied as a natural response of the solar flares in their vicinity regions (Roberts, Edwin, and Benz, 1983; Aschwanden *et al.*, 1999; Wang *et al.*, 2002; Foullon *et al.*, 2005; Ballai, Erdélyi, and Pintér, 2005; Nakariakov *et al.*, 2006; Taroyan *et al.*, 2007; Erdélyi and Taroyan, 2008). The energy deposited in these MHD oscillations are found to be orders of magnitude smaller compared to the flare energy

release (Terradas, Andries, and Goossens, 2007). On the other hand, flare and CME induced waves and oscillations are also very useful to gain first insight into the local plasma conditions and dynamical processes of the active regions (Erdélyi and Verth, 2007; Andries *et al.*, 2009; Aschwanden, 2009; Taroyan and Erdélyi, 2009; Terradas, 2009; Ofman, 2009; Ruderman and Erdélyi, 2009).

In addition to the large-scale motions in terms of flows and ejecta, waves and oscillations of magneto-fluids, and energetics of solar eruptions, the formation of small-scale plasma motions, e.g., anemone jets, spicules, penumbral jets (De Pontieu, Erdélyi, and James, 2004; De Pontieu and Erdélyi, 2006; De Pontieu *et al.*, 2007; Katsukawa *et al.*, 2007; Kumar, Srivastava, and Dwivedi, 2011), waves in form of transient pulses and wave-packets (Zaqarashvili, Kukhianidze, and Khodachenko, 2010; Murawski and Zaqarashvili, 2010; Srivastava and Dwivedi, 2010) are important in observations to understand the heating and dynamics of the solar plasma at small spatio-temporal scales. These MHD/HD pulses may also be important to power small-scale transients in the lower solar atmosphere (Murawski and Zaqarashvili, 2010). The theory of MHD pulses and wave excitation are somewhat established (Roberts and Webb, 1979; Carlsson, Judge, and Wilhelm, 1997; Selwa and Ofman, 2010; Selwa, Ofman, and Murawski, 2007; Murawski and Zaqarashvili, 2010). However, observational signatures are not very abundant in past few years to understand their role in the excitation of solar transients (e.g., jets at various spatio-temporal scales). On the other hand, the role of magnetic reconnection, twisted flux emergence from sub-photospheric layers, and generation of instabilities are well-studied both in observations and theories in the jet productive regions (Culhane *et al.*, 2007; Nishizuka *et al.*, 2008; Filippov, Golub, and Koutchmy, 2009; Pariat, Antiochos, and DeVore, 2009).

In the present paper, we analyze multi-wavelength imaging data of the Active Region NOAA AR 10808 that has produced violent explosions in the form of giant solar flares and associated eruptions. However, this active region has exhibited a very interesting phenomena, surprisingly rather quietly before an M-class flare on 9 September 2005, in the form of a supersonic cylindrical plasma blob ejection from the flare site between 05:27 UT and 5:33 UT. The blob was observed by TRACE 171 Å and also in H α image sequences captured by Culgoora Solar Observatory, Australia. We present the observational data in Sec. 2. A numerical modelling and the theoretical interpretations of the supersonic plasma blob is described in Sec. 3. The results and discussions are given in the last section.

2. Observations of Supersonic Plasma Blob

Active Region NOAA 10808 has appeared on the east limb on 07 September 2005 and produced at least 10 X-class and 25 M-class solar flares until it disappeared behind the solar-disk (Nagashima *et al.*, 2007). The active region was located nearby the eastern limb of the southern hemisphere near the equatorial plane at S10E67 with $\beta\gamma\delta$ field configuration of the sunspot group. This active region was also associated with CMEs and filament eruptions, and produced numerous space weather activities by its furious eruptive events (Archontis and Hood, 2010; Canou *et al.*, 2009; Nagashima *et al.*, 2007; Wang *et al.*, 2006; Li *et al.*, 2007). Figure 1 shows the coronal image of AR 10808

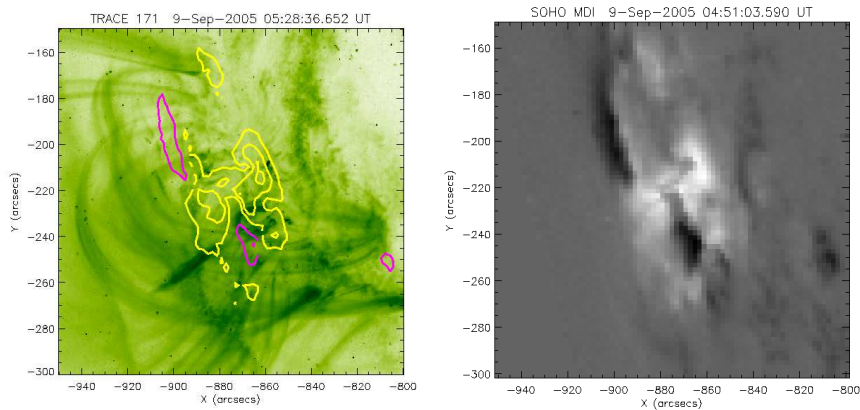


Figure 1. Field-of-views : Co-aligned MDI contours overlaid on TRACE 171 Å context image of the Active Region 10808 at 05:28:36 UT on 9 September, 2005 (left-panel). Yellow (magenta) contours show the positive (negative) polarity of the photospheric magnetic field. The maximum level of the magnetic field contours are ± 4000 G. For the positive polarity, the two concentric iso-contours of magnetic fields are visible. The plasma blob is shown to be propagating up in the solar atmosphere from its origin site associated with maximum magnetic fields. The observed configuration of the active region magnetic field is shown in the right panel on 04:51 UT, which later comes more inside the disk during the transient event.

as observed from the TRACE 171 Å filter at 05:28:36 UT on 09 September, 2005. The TRACE field of view is overlaid by co-aligned MDI contours showing positive (yellow) and negative (magenta) magnetic polarities (left panel of Figure 1). The positive and negative polarities seem to be elongated respectively towards north-west to south-east, and north-east to south-west, with tongue-like structures (cf., right panel of Figure 1). This is a very typical signature of AR10808 and seems to be the evidence of the emergence of twisted rising flux (Archontis and Hood, 2010; Li *et al.*, 2007). This typical characteristic of the AR10808 was one of the main causes that were responsible for the very energetic flares, CMEs, and filament eruptions, though the rotation of spots and the tilt of the bipolar weightage axis were also observed in this active region (Archontis and Hood, 2010; Canou *et al.*, 2009; Nagashima *et al.*, 2007; Wang *et al.*, 2006; Li *et al.*, 2007). Although the violent solar eruptions have been extensively analyzed from this active region, we highlight here an additional and an interesting plasma dynamics during an M-class flare that took place for a short duration of about 5-7 minutes on 9 September 2005. The M6.2 class solar flare has occurred in AR10808 at the location S10E66. It starts at 05:32 UT, peaks at 05:48 UT, and ended at 06:00 UT. The observed short duration plasma dynamics that is the interest and theme of this paper, has occurred well before this M6.2 class solar flare just at the flare brightening site.

Figure 2 shows the time series of TRACE 171 Å images of the flaring region in AR10808 during the time interval 05:24-05:29 UT. The plasma blob (a dark and dense material) is formed between 05:24-05:27 UT above the flare site, followed by its detachment and propagation upward after 05:27 UT. TRACE has missed the later part of the observations that is, however, captured by H α observations from Culgoora Solar Observatory (cf., Figure 4). The length and width of

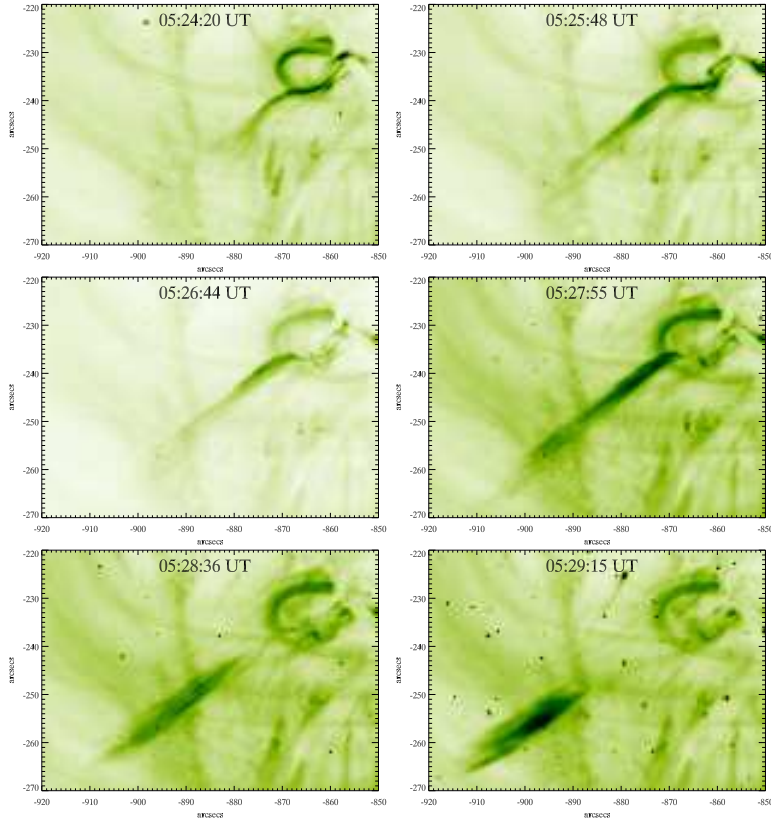


Figure 2. Selected series of TRACE 171 Å images in negative colors showing a moving blob structure above the smaller bright loop of AR10808.

the plasma blob, as observed in the TRACE images in its dynamic phase, are approximately as 22 Mm and 5 Mm, respectively. The blob is co-spatially and contemporarily visible in the TRACE 171 Å and H_{α} (6563 Å) emissions, and finally vanishes around 05:33 UT. In the TRACE snapshot at 05:27:55 UT, the tail of the eruptive plasma was rooted at $(X_1, Y_1) \approx (-867'', -236'')$, while at 05:28:36 UT it reaches at $(X_2, Y_2) \approx (-880'', -247'')$. Therefore, the projected distance d_{12} covered in $\Delta t_{12} \approx 41$ s is $\approx 12,346$ km. Thus, the approximate apparent speed (v_1) derived from these two snapshots is ≈ 300 km s^{-1} . At 05:29:15 UT, the tail of the blob that is almost constant in shape for around 3-4 mins, reaches at $(X_3, Y_3) \approx (-888'', -250'')$. Therefore, the distance d_{23} covered in $\Delta t_{23} \approx 39$ s is ≈ 6200 km. Assuming the $1'' = 725$ km scale for the conversion, therefore, derived approximate speed (v_2) is ≈ 160 km s^{-1} that can be obtained as the blob propagates. Therefore, the average speed of travel is $v_{av} = (v_1 + v_2) / 2 \approx 230$ km s^{-1} . After this the blob quickly vanishes in the corona. Note that the measured speeds v_1 and v_2 are projected speeds of the blob by tracing its detached tail, and the actual speeds may be higher compared to the estimated speeds. Also worth illustrating that these speeds are anyway higher when compared to the local sound-speed (~ 150 km s^{-1}). Next, we trace the approximate position of

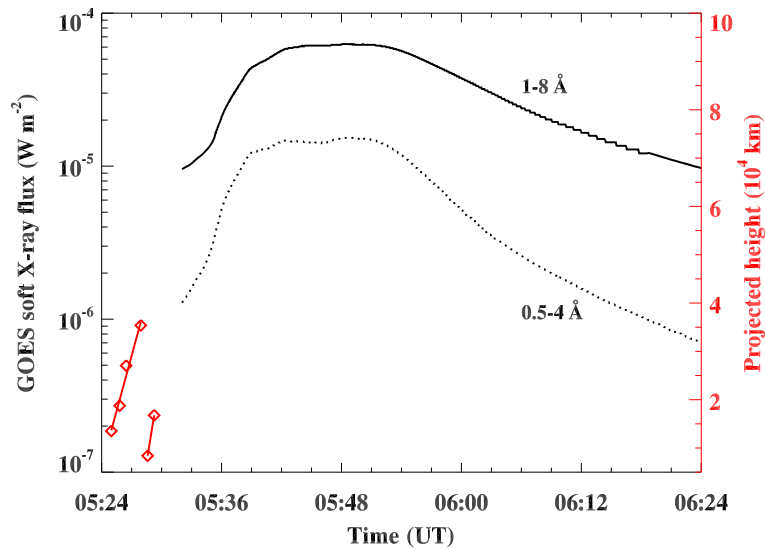


Figure 3. The GOES X-ray profiles show a long duration M-class flare, and its temporal relation with the rising of plasma blob. The initiation and dynamic phases of rise-up are linearly fitted to derive the projected lower bound speeds. The upper and lower linear fits represent, respectively, the initiation and dynamical phase of blob under the observational baseline of TRACE data. The linear fit between 05:24-05:27 UT corresponds to the position of the leading edge of the blob while the fit at 05:28-05:30 UT shows the position of its trailing edge.

the core of the moving feature in its dynamic phase to find its projected speed as $\approx 175 \text{ km s}^{-1}$. Since it is very difficult and somewhat superfluous also to track the diffused and faint head of the moving feature, therefore, we only take the references of the core and tail of blob observed in the TRACE images to estimate the approximate lower bound speeds. In conclusion, the blob plasma moves almost collectively after its origin and detachment from the flaring site due to reconnection. In the TRACE snapshots during 05:24 UT-05:27 UT, it is clear that there is some interaction of the rising plasma column that has detached later on in form of a blob, with the pre-existing fields. The magnetic field configuration becomes simpler (cf., 05:28-05:29 UT snapshots) at the origin site of the blob after its detachment.

Next, the Figure 3 shows the GOES soft X-ray evolution of the M6.2 class solar flare observed in the active region and the corresponding projected time-distance plot of the observed plasma blob in its initiation and dynamic phase during 05:24-05:35 UT is also co-plotted. This is very clear that the blob rises in a plasma column with a rather low subsonic speed in its build-up phase (cf., upper linear fit in Figure 3), however, it accelerates in the dynamic detached phase to a speed of 215 km s^{-1} that crosses the sonic speed level and propagation becomes supersonic (cf., lower linear fit in Figure 3). We found that, meanwhile, two more eruptions have been occurred, respectively, at 05:15 UT and 05:50 UT from the same location (see the attached movie trace-eruptions.avi), however, they are exclusively different from the observed unique plasma blob. Firstly, other eruptions do not propagate in a definite shape of a blob, and secondly they are

not visible simultaneously in the cool $H\alpha$ temperature. However, the multiple supersonic eruptions from the same location may be the collective signature of repetitive reconnections ongoing at the flare site. Figure 3 also depicts the linear fit in the projected distance of the travel of blob as measured from the TRACE image sequence, and it is also given both in its initiation and detached dynamic phases. The linear fit between 05:24-05:27 UT corresponds to the position of the leading edge of the blob in the initiation phase, while the fit at 05:28-05:30 UT shows the position of its trailing edge in the dynamical phase. The speed measured in the dynamical phase matches well with the average speed of 230 km s^{-1} as measured crudely by analyzing TRACE image sequence. We note that the plasma column was built well before the flare event, while the dynamic phase of the blob is achieved just before the rising phase of the flare. The rising speed of the plasma column before the detachment of the blob is $\approx 126 \text{ km s}^{-1}$ before the occurrence of the flare event. This phase of the rising of plasma column is clearly evident in Figure 2 during 05:24-05:28 UT. The denser and brighter material is also filled in the plasma column during this time span, which later detached in form of the observed plasma blob. We measure the speed of the rise-up of this plasma column in the initiation phase before the detachment of blob by tracing its leading edge during the course of time (cf., snapshots during 05:24-05:28 UT in Figure 2, and upper linear fit in Figure 3). While in the dynamic phase, the blob gains a supersonic speed of $\approx 215 \text{ km s}^{-1}$ as per the linear fit measurements, during early rising phase of the gradual M-class solar flare. This measured speed is now much more accurate measurement. The average sound speed at the Fe XI 171 \AA formation temperature ($T_f = 1 \times 10^6 \text{ K}$) is $\sim 150 \text{ km s}^{-1}$. Therefore, the blob propagates with a supersonic speed, quickly changes its shape, and finally becomes fainter against the background by most likely dissipating its energy and material draining back to the low atmosphere (see the movie trace-eruptions.avi). It should be noted that the whole process has two phases: first the initiation phase in which the plasma column and associated cylindrical plasma blob is build-up, followed by the second dynamical stage when the plasma blob become detached and moves up in the corona with a supersonic speed within few minute time scale. The true speed (projected) what is quoted here is in the dynamical phase and is consistent both with $H\alpha$ and TRACE observations.

The $H\alpha$ observations of this active region was carried out at Culgoora Solar Observatory at Narrabri, Australia by using a 12 cm f/15 Razdow solar patrol telescope equipped with an $H\alpha$ filter of the Lyot type that has a pass bandwidth of 0.5 \AA . The raw images were recorded by an 8 bit 1024×1024 pixels CCD camera system with pixel size $6.7 \times 6.7 \mu\text{m}^2$. The spatial resolution of the camera is $2''$ per pixel. The typical cadence for the present observations is at least 1 frame per minute. The observations are carried out with a FOV of the full-disk solar image. Figure 4 shows a sequence of data of the propagating blob emphasized by a yellow arrow from AR10808 before an M-class flare during 05:26 UT–05:36 UT. The difference images of Figure 4 are a $160'' \times 100''$ partial field of view provided to us by Culgoora Solar Observatory under its data use policy. Although, the resolution of the images is not very high, it should be noted that this is the only $H\alpha$ observations that are available from the ground as this unique event occurred in its day-light time zone. The temporal $H\alpha$ observations are thus very

useful and show the unique signature of the propagation of a *low-temperature* counterpart of the plasma blob observed by TRACE propagating away from the flare site towards the eastern limb in a projection. A careful investigation of the H_α image sequence shows that the blob is initially of a cylindrical shape of the length of ≈ 22 Mm and width of ≈ 5 Mm. The length and width are found to be consistent with the observed TRACE images in the dynamic phase of the blob. Therefore, we conclude that initially the length to width ratio is 4.4. It should also be noted that not only the position but also the length to width ratio may also be influenced by projection effects. The blob changes its shape quickly and is faded within 4-5 minutes of its evolution as visible in H_α at 05:28 UT. The measured lower bound speed of this propagating blob is found to be ~ 200 km s^{-1} . This is again the projected speed of the blob, and the actual speed may be higher compared to this lower bound estimated speed. The average sound speed of the H_α formation temperature ($T_f = 1 \times 10^4$ K) is 15 km s^{-1} . Therefore, the blob propagates with supersonic speed.

3. Theoretical Modelling and Interpretation

As we have explained in the previous section, the analyses of the H_α and TRACE 171 Å temporal data between 05:24 UT–05:36 UT well before an M6.2 class flare from AR10808 on 9 September 2005 show the observational evidence of the supersonic plasma blob that propagates in the higher solar atmosphere with a supersonic speed of ~ 215 km s^{-1} . We firstly explore the possibility of the generation of this supersonic blob as a reconnection-generated plasmoid. The observed blob may be the plasmoid as recorded previously by Manoharan and Kundu (2003) due to magnetic reconnection during the rising phase of an M-class flare. They have observed the motion of plasma blobs associated with a sigmoid, Moreton wave, CME injection in the interplanetary space, and associated radio bursts from AR9393 on 2 April 2001 at 11:00 UT. They have also found magnetic reconnection around a coronal null point as a cause of such eruptions and associated phenomena. Recently, the multiple plasmoid and its dynamics have also been observed in solar flares (Bárta, Karlický, and Žemlička, 2008; Nishizuka *et al.*, 2010). However, such plasmoids are the high-speed plasma blobs that accelerate outwards the reconnection point in the solar atmosphere and usually are associated with the rising phase of the solar flares. These plasmoids are often released with CME ejections, supersonic down-flows that causes the HXR emissions, and radio bursts (Manoharan and Kundu, 2003). In the present case, the supersonic blob is observed well *before* the M 6.2 class flare, and there is no observational evidence of associated CMEs and radio bursts even in this most violent super-active region associated with this flare on 9 September 2009. Kundu *et al.* (2001) have reported that the plasmoid ejecta are associated with metric/decimetric emission that starts significantly after the impulsive hard X-ray (20 keV) and microwave bursts. In this event, however, we do not observe any metric/decimetric or microwave radio emissions as evident in the Culgoora and Learmonth radio spectra, and no impulsive hard X-ray emissions are evident at that time as per RHESSI X-ray flux profiles. These observed facts possibly

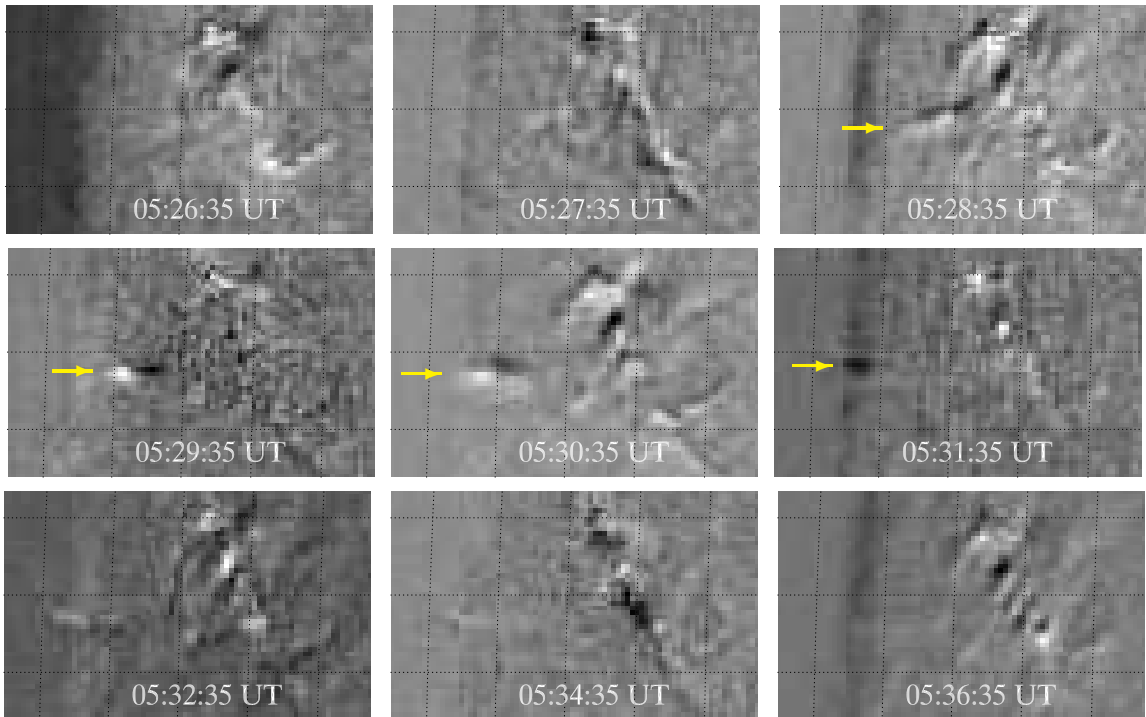


Figure 4. Selected H_{α} difference images obtained from H_{α} observations of the Culgoora Solar Observatory showing a moving blob structure towards the eastern limb highlighted by yellow arrow. The size of each image is $160'' \times 100''$.

exclude the formation and acceleration of the supersonic plasmoid excitation in our case. In conclusions, although the morphology of the observed blob and its dynamics are not favorable for the plasmoid ejection, sometime it may be difficult to distinguish between the plasma blob formed by the reconnection rate change and real plasmoids (Bárta *et al.*, 2007). The detailed analyses of the magnetic field topology can only differentiate between these two. Moreover, a single plasmoid does not need to be accompanied with radio/HXR emissions always. The most likely interaction of multiple plasmoids may be responsible for particle acceleration and related emissions.

The observed plasma blob may be a reconnection-generated jet as per its typical length, time, velocity scales of the coronal jets (Nisticò *et al.*, 2009). However, we suggest that the observational evidences point towards more in the form of a pulse driven blob, which may be a special type of detached jet rather than a classical jet-like structure. Secondly, the blob is visible both in H-alpha and TRACE 171 Å with similar shape and dynamics, which indicate that it is formed by *multi-temperature* plasma. The bi-directional EUV jets (Innes *et al.*, 1997) are the natural consequences of the flow induced coronal X-type reconnections as theorized by many workers (Petschek, 1964; Roussev *et al.*, 2001). However, the various types of the classical EUV jet as well as such type of observed plasma packets that move radially outwards from the lower solar atmosphere, can either

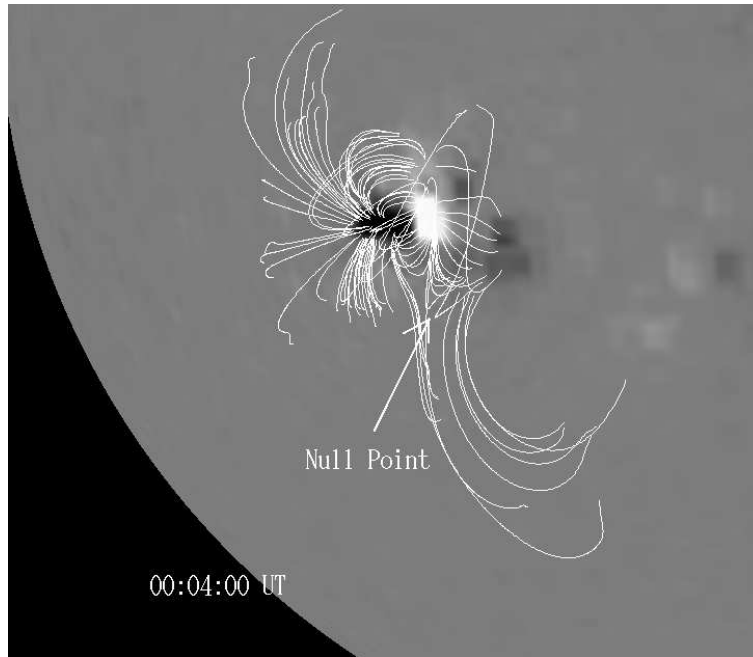


Figure 5. Potential Field Source Surface (PFSS) extrapolation overplotted on the MDI map of 00:04 UT at 9 September 2005 shows the configuration of overlying loops and the position of magnetic null point.

be a direct consequence of the low-atmospheric reconnection of the low-lying loop systems (Nisticò *et al.*, 2009) or the energy build-up due to some magnetic instabilities (Patsourakos *et al.*, 2008). Therefore, the observed blob may also be the consequence of the low-atmospheric reconnection as also evident in the observations.

If the supersonic blob is not a typical form of the ejecta of flaring active regions, e.g., reconnection-generated classical jets, plasmoids etc, then the question arises about its identification and the most probable drivers during its initiation and dynamic phases. Recently Zaqarashvili, Kukhianidze, and Khodachenko (2010) have reported the propagation of sausage solitons in the quiet Sun chromosphere using Hinode/SOT observations. They have reported the propagation of a supersonic plasma blob in the solar chromosphere, which retain the almost constant shape (length to width ratio) and obeys the soliton solution. The propagating blob reported in this paper here also moves with a supersonic speed, but changes its relative intensity amplitude as well as the shape (length to width ratio) within 3 minutes of its launch at 05:27 UT and, then, quickly vanishes against the background plasma. Therefore, the soliton description is not the most evident and plausible explanation associated with the observations reported here.

The interpretation of a kink pulse/wave may be another possibility to drive such observed plasma blob/jet in its dynamic phase (Kukhianidze, Zaqarashvili, and Khutsishvili, 2006; Cirtain *et al.*, 2007). However, the axial transversal displacements or a curved form of the pulse is not evident in the observations. The density and thus in-

tensity enhancement in the associated inclined flux tube is also not evident as reported by Cooper, Nakariakov, and Williams (2003). Therefore, the possibility of the kink pulse as a driver of the supersonic blob in its dynamic phase, is also out of the scope under the baseline of the observations. Another and perhaps the most plausible possibility is then the excitation of a fast MHD pulses/wave train in the flaring active region as a manifestation of the supersonic blob in its dynamic phase. The blob propagates with supersonic speed and vanishes quickly in the corona within 3-4 minutes. The blob may be energized by the fast wave trains generated in the solar atmosphere (Nakariakov *et al.*, 2004). In such a case, we should observe the quasi-periodic multiple rise and fall of the blob material, which is indeed not evident in the observations presented in the paper. Therefore, the fast MHD pulse train is an unlikely driver for the observed supersonic plasma blob made-up by the multi-temperature plasma. In conclusion, the observed blob is neither some classical phenomena of the solar atmosphere (e.g., Y-shaped typical jets, plasmoids, up-flows etc), nor it is the signature of the peculiar MHD phenomena (e.g., sausage solitons, fast MHD wave trains, kink pulses etc).

Therefore, we suggest that the reconnection-generated velocity pulse at flaring site may be the most likely driver of the plasma blob. The energy release at reconnection site in the lower solar atmosphere perturbs the plasma velocity and most possibly creates a velocity pulse that trigger the plasma eruption in the form of a supersonic blob. To the best of our knowledge, this is the first observational signature of the excitation of a velocity pulse driven supersonic plasma blob in the solar atmosphere above an active region in the vicinity of a flare site. The most likely possibility is that the low-lying magnetic loops reconnect with each other. This reconnection is at its beginning in the steady state and most probably with a single dissipation region. Since, this reconnection region has so far not reached its dynamical state with many plasmoids created, therefore, low number of particles is accelerated and we do not observe either radio or HXR emission. Hence, this steady reconnection gives only the rise of the plasma jet which we observe from the very beginning (e.g., Figure 2, 5:24 UT snapshot). The formation of the plasma jet during steady state reconnection further changes into the detached blob propagating in corona. As the reconnection rate and reconnection regime change, a velocity pulse may be generated to accelerate the plasma blob. Due to the mass conservation, a density blob is formed in the outflow jet, which detaches from the reconnecting loops and propagates upwards until it vanishes in the solar corona.

We also explore the details of magnetic field topology to understand the most possible generation of such plasma dynamics that we have been observed. The magnetic field configuration and topological distribution of its positive and negative polarities are shown in Figure 1. It is clear from Figure 1 that the positive polarity region is stretched towards the west with a remote tongue, while the negative polarity is stretched towards the east with a remote tongue in the opposite direction as an indicator of the emergence of the twisted magnetic fluxes (e.g., Archontis and Hood, 2010; Li *et al.*, 2007). The Potential Field Source Surface (PFSS) extrapolation (Figure 5) of the SoHO/MDI at 00:04 UT on 09 September 2005 also reveals the formation of a coronal null point above a

positive polarity sunspot which is joining the two segments of oppositely lying negative polarities by bipolar loop systems. This is a very preliminary configuration of the AR magnetic field well before the event, and later phase was also associated with the high flux-emergence and build-up of the complexity in the region (cf., Figure 1, right-panel). This configuration might force the steady state magnetic reconnection in the lower part of the atmosphere. The PFSS is slightly shifted in its centroids so that we see clearly the extrapolated field and its configuration more towards our line-of-sight. In this parasitic region, the central positive polarity spot is a unipolar flux region and connecting with the two opposite polarity regions on both sides. This is similar situation as the formation of a dome-like fan surface where the symmetry axis is known as spine containing a null point at the intersection with the fan dome (Aschwanden, 2004). Our observations (Figure 5) show a clear evidence of the formation of a parasitic region, i.e., the fan dome, null-point and spine at the flare site in the active region. However, the energy release may be taking place well below this magnetic null point due to pre-emergence and therefore the reconnection process with the existing field lines in the lower solar atmosphere. The field topology in Figure 5 is following the standard magnetic topology of a 3-D reconnection process via a separator dome (see Figure 10.27 of Aschwanden, 2004 and Fletcher et al., 2001). The PFSS extrapolation schematic diagram (extrapolated field lines over SoHO/MDI image) approximately matches well with the standard scenario of the 3-D reconnection and thus the re-arrangements of the field lines and mass motion along open field lines in the vicinity of the null point. However, it seems that the steady state reconnection generates the plasma jet in the lower solar atmosphere. There may be some small energy release also during the magnetic field rearrangements of the dynamical reconnection process, however, it is clear that there is no bulk heating of the plasma before achieving the flare maximum. Moreover, there is no expansion or diffusion of the detached plasma along the field lines outward. Therefore, we discard the acceleration of the blob due to the generation of a thermal pulse by bulk heating. This magnetic field re-arrangements during the reconnection process is found to be the driver of a velocity pulse along the radial direction outward and the observed driven supersonic plasma blob. This type of reconnection scenario drives the plasma outward in the radial direction along the spine-lines due to the low-atmospheric reconnection between the low-lying loop systems. This reconnection generates a velocity pulse, which associates with a shock steepened in the corona to drive the plasma blob. Therefore, we have the consistent observation of an uni-directional detached jet or plasma blob propagating outwards. Recently, the reconnection-generated velocity pulse driven jet (Srivastava and Murawski, 2011), and macrospicules (Murawski, Srivastava, and Zaqarashvili, 2011) have already been modeled. However, this is the first attempt to numerically model the reconnection generated and velocity pulse driven plasma blob in the solar corona.

Here, the most generic and real situation is that the plasma blob is launched due an initial radial velocity pulse along the magnetic field lines at the triggering site of the blob. The blob is generated approximately 5-6 Mm above the photosphere with the start of the reconnection process. The reconnection at this height in the low-lying quadrapolar loop system may generate the velocity pulse

which may cause the formation of the supersonic plasma blob propagating up in the corona. In the next section, we model numerically the propagation of the supersonic plasma blob generated by a velocity pulse at the reconnection site.

3.1. Numerical simulations

We consider a gravitationally stratified solar atmosphere which is described by the ideal 2D magnetohydrodynamic (MHD) equations:

$$\frac{\partial \varrho}{\partial t} + \nabla \cdot (\varrho \mathbf{V}) = 0, \quad (1)$$

$$\varrho \frac{\partial \mathbf{V}}{\partial t} + \varrho (\mathbf{V} \cdot \nabla) \mathbf{V} = -\nabla p + \frac{1}{\mu} (\nabla \times \mathbf{B}) \times \mathbf{B} + \varrho \mathbf{g}, \quad (2)$$

$$\frac{\partial p}{\partial t} + \nabla \cdot (p \mathbf{V}) = (1 - \gamma) p \nabla \cdot \mathbf{V}, \quad p = \frac{k_B}{m} \varrho T, \quad (3)$$

$$\frac{\partial \mathbf{B}}{\partial t} = \nabla \times (\mathbf{V} \times \mathbf{B}), \quad \nabla \cdot \mathbf{B} = 0. \quad (4)$$

Here ϱ is the mass density, \mathbf{V} the flow velocity, \mathbf{B} the magnetic field, p the kinetic gas pressure, T temperature, $\gamma = 5/3$ the adiabatic index, $\mathbf{g} = (0, -g)$ the gravitational acceleration where $g = 274 \text{ m s}^{-2}$, m denotes the mean particle mass and k_B the Boltzmann's constant.

We assume that the solar atmosphere is in static equilibrium ($\mathbf{V}_e = 0$) with a force-free magnetic field, $(\nabla \times \mathbf{B}_e) \times \mathbf{B}_e = 0$. At this equilibrium the pressure gradient is balanced by the gravity force, $-\nabla p_e + \varrho_e \mathbf{g} = 0$. Here the subscript 'e' corresponds to equilibrium quantities. Using the ideal gas law and the y -component of hydrostatic pressure balance, we express the equilibrium gas pressure and mass density as

$$p_e(y) = p_0 \exp \left[- \int_{y_r}^y \frac{dy'}{\Lambda(y')} \right], \quad \varrho_e(y) = \frac{p_e(y)}{g \Lambda(y)}. \quad (5)$$

Here $\Lambda(y) = k_B T_e(y)/(mg)$ is the kinetic pressure scale-height, and p_0 denotes the kinetic gas pressure at the reference level that we choose in the solar corona at $y_r = 10 \text{ Mm}$. We adopt an equilibrium temperature profile $T_e(y)$ for the solar atmosphere that is close to the VAL-IIIC atmospheric model of Vernazza, Avrett, and Loeser (1981).

We assume that the initial magnetic field satisfies a current-free condition, $\nabla \times \mathbf{B}_e = 0$, and it is specified by the magnetic flux function, A , such that $\mathbf{B}_e = \nabla \times (A \hat{\mathbf{z}})$. We set an arcade magnetic field by choosing

$$A(x, y) = B_0 \Lambda_B \cos(x/\Lambda_B) \exp[-(y - y_r)/\Lambda_B]. \quad (6)$$

B_0 is the magnetic field at $y = y_r$, and the magnetic scale-height is $\Lambda_B = 2L/\pi$. We use $L = 30 \text{ Mm}$.

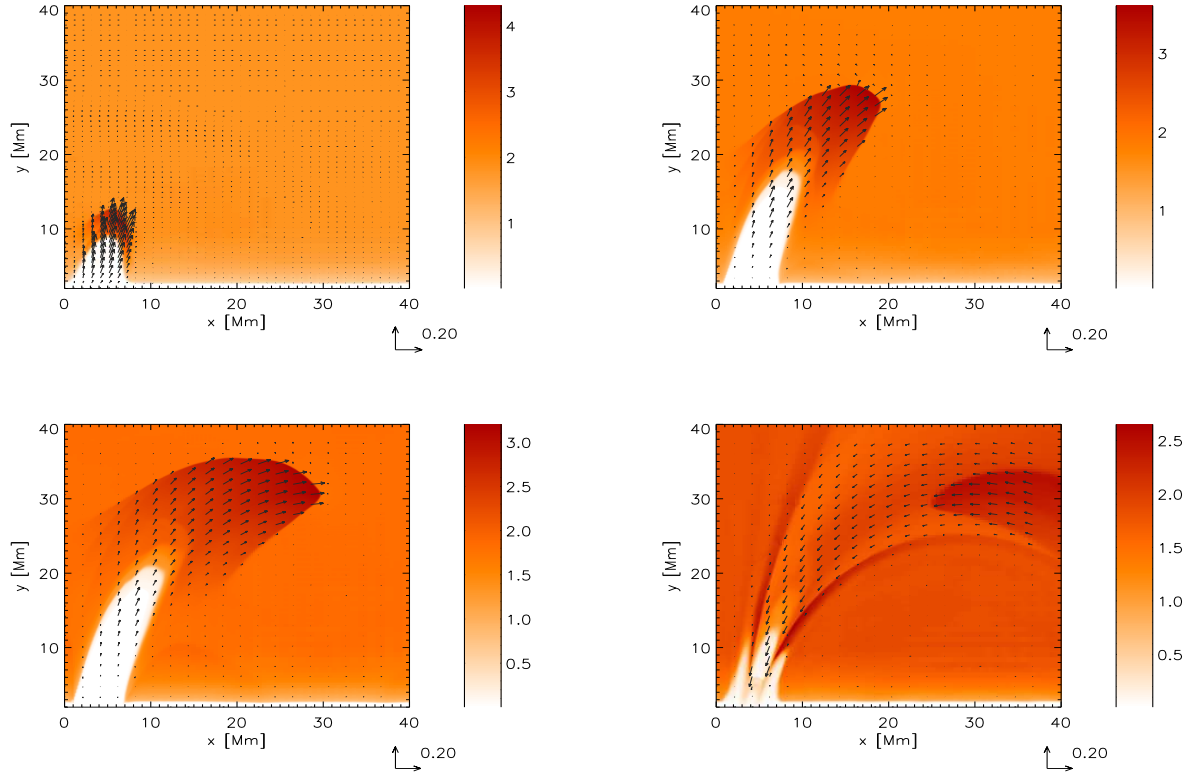


Figure 6. Numerical results : Temperature (colour maps) and velocity (arrows) profiles at $t = 25$ s, 100 s, 150 s, and 600 s (from left-top to right-bottom). Temperature profiles are drawn in units of 1 MK. The arrow below each panel represents the length of the velocity vector, expressed in units of 200 km s^{-1} .

We initially perturb the above equilibrium impulsively by a Gaussian pulse in the vertical component of velocity, V_y , viz.,

$$V_y(x, y, t = 0) = A_v \exp \left[-\frac{(x - x_0)^2 + (y - y_0)^2}{w_p^2} \right]. \quad (7)$$

Here A_v is the amplitude of the pulse, (x_0, y_0) is its initial position and w_p denotes its width. We choose and hold fixed $x_0 = 4 \text{ Mm}$, $y_0 = 5 \text{ Mm}$, $w = 2 \text{ Mm}$, and $A_v = 300 \text{ km s}^{-1}$.

Equations (1)-(4) are solved numerically using the code FLASH (Lee and Deane, 2009). This code implements a second-order unsplit Godunov solver with various slope limiters and Riemann solvers, as well as adaptive mesh refinement (AMR). We set the simulation box of $(-2.5, 65) \text{ Mm} \times (2, 45.5) \text{ Mm}$ along the x - and y -directions and impose fixed in time all plasma quantities at all four boundaries of a simulation region. In all our studies we use AMR grid with a minimum (maximum) level of refinement set to 4 (7). The refinement strategy is based

on controlling numerical errors in temperature. Every block consists of 8×8 identical numerical cells.

Figure 6 displays the spatial profiles of plasma temperature (colour maps) and velocity (arrows) resulting from the initial velocity pulse which splits into counter-propagating parts. As the plasma is initially pushed upwards the under-pressure results in the region below the initial pulse. This under-pressure sucks up cold photospheric plasma which lags behind the shock front. The pressure gradient force works against gravity and forces the chromospheric material to penetrate the solar corona. At $t = 25$ s this shock reaches the altitude of $y \simeq 10$ Mm. The next snapshot (top right panel) is drawn for $t = 100$ s. At this time the shock reached the altitude of $y \simeq 30$ Mm while the cold plasma blob is located at $y \simeq 18$ Mm. By the next moment of time (bottom left panel) the shock has already moved up to the right boundary and the cool counterpart of blob exhibits its developed phase. This is also evident in the H_α and TRACE observations that a cool core of 10,000 K and hot coronal plasma maintained at 1-2 MK temperature are simultaneously present in the plasma blob. The shock-heated supersonic plasma as well as the cool counterpart both disappear in the corona at $t = 600$ s (bottom right panel). This matches well the observations. The blob already subsided and the plasma began to flow downward, being attracted by gravity. In the present simulation, we only assume the reconnection as a cause that effectively generates the radial velocity pulse. We do not invoke the reconnection generated joule heating in our model as it can generate the thermal pulse in the ambient medium of certain spatio-temporal scale that can launch the heated plasma in the upward magnetized atmosphere above the reconnection region (Srivastava and Murawski, 2012). Therefore, our model takes the flexibility to not consider any initial conditions generated by reconnection, and we initiate with the launch of the radial velocity pulse triggered due to reconnection process. We do not invoke therefore either the heating or the losses due to thermal conductivity and radiation in our model. The inclusion of these factors will be of the subject of our future study.

Figure 7 displays the spatial profiles of plasma density (colour maps) and velocity (arrows) resulting from the initial velocity pulse which splits into counter-propagating parts. In the snapshot (top right panel) drawn for $t = 100$ s, the shock reached the altitude of $y \simeq 30$ Mm while the denser cool plasma blob is located at $y \simeq 18$ Mm. By the next moment of time (bottom left panel) the shock has already moved up to the right boundary and the cool counterpart of blob exhibits its developed phase. This is also evident in the H_α and TRACE observations that a cool and denser core of 10,000 K and comparatively less denser hot coronal plasma maintained at 1-2 MK temperature are simultaneously present in the plasma blob. These findings of numerical simulation validate our multi-wavelength observations of detached blob shaped jet upto some extent. The shock-heated supersonic plasma as well as cool counterpart both disappear in the corona at $t = 600$ s (bottom right panel) that matches well with the observations. The blob already subsided and the plasma began to flow downward, being attracted by gravity. However, the clear-cut detachment of the blob material from its origin point is not visible as clearly as in the observations.

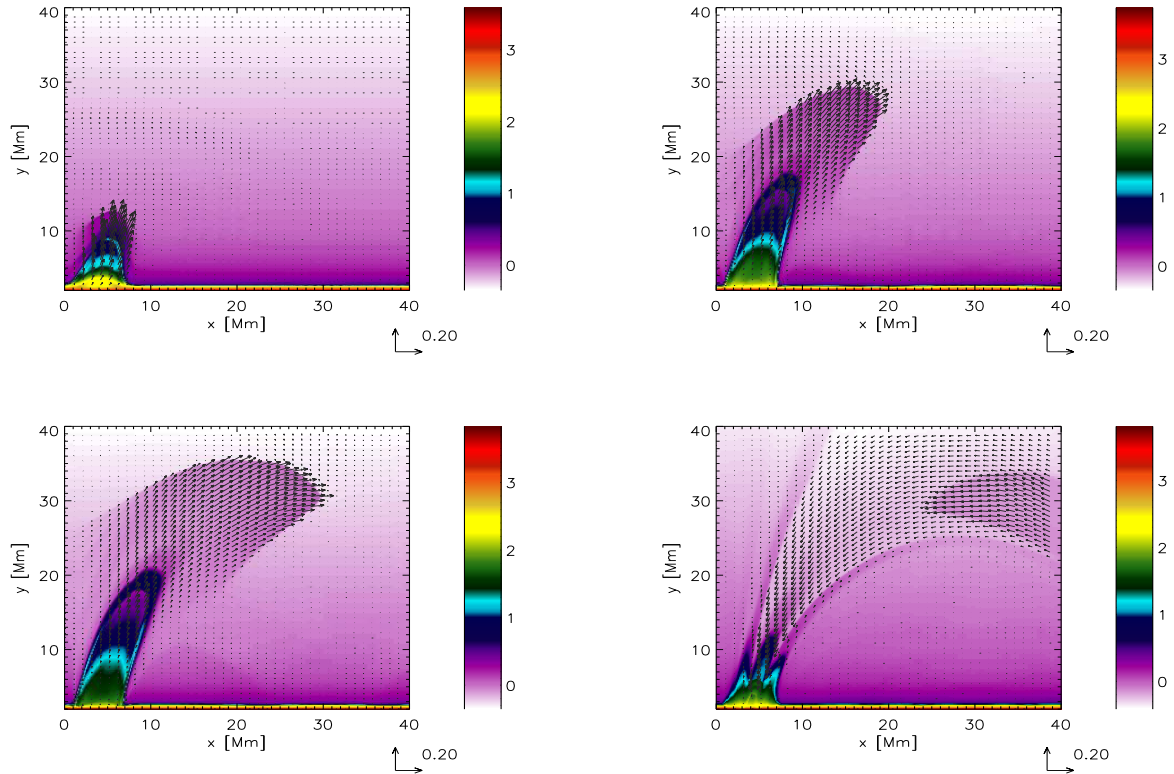


Figure 7. Numerical results : Density (colour maps) and velocity (arrows) profiles at $t = 25$ s, 100 s, 150 s, and 600 s (from left-top to right-bottom). Density is drawn in logarithmic density scales. The arrow below each panel represents the length of the velocity vector, expressed in units of 200 km s^{-1} .

Figure 8 illustrates the relative mass density $(\rho - \rho_e)/\rho_e$, that is collected in time at the detection point ($x = 20, y = 30$) Mm for the case of Figure 7 that mimic the observed blob-shaped detached jet. As a result the mass falls off with height and upwardly propagating waves steepen rapidly into shocks. The arrival of the first shock front to the detection point is at $t \simeq 115$ s. The second shock front reaches the detection point at $t \simeq 865$ s, i.e., after ~ 750 s. This secondary shock results from the reflected wave from the transition region. Therefore, the observation of the intensity (thus density) variations in the detached phase of the blob as evident in $\text{H}\alpha$ and TRACE, is due to the variation of density in the plasma blob by the periodic steepening of velocity pulse.

4. Discussion and Conclusions

Using multi-wavelength observations from TRACE 171 Å MDI/SoHO, and $\text{H}\alpha$ from Culgoora Solar Observatory, we have observed a supersonic plasma blob

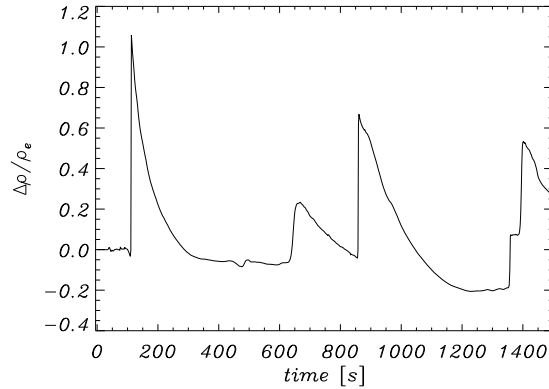


Figure 8. Time-signatures of perturbed mass density collected at $(x = 20, y = 30)$ Mm for the case of Figure 7. Time t is expressed in units of 1 s.

just before M6.2 class flare in AR 10808 on 9 September 2005. The blob moves with a supersonic speed of $\sim 215 \text{ km s}^{-1}$ in its dynamical phase and quickly vanishes in the corona. The supersonic speed, vanishing nature, increment of the intensity (thus density) followed by its decrement during the life-time of blob, all collectively support the excitation of a velocity pulse just in the vicinity of the magnetic null point and reconnection is suggested to be a primary driver. At the same place, the repetitive plasma dynamics at 05:15 UT, and 05:50 UT have also been observed. However, they were much fainter and the blob shape plasma eruption was not evident in those processes. Moreover, those eruptions were also not visible in the cool $\text{H}\alpha$ temperature. Therefore, we have a unique observational signature of the propagation of a supersonic plasma blob during the multiple plasma eruptions at the flare site in AR 10808. This is the most likely clue of the occurrence of the repetitive reconnection processes in the observed active region well before and near to M-class flare, which generates the multiple plasma eruptions as well as the supersonic blob, which may also be a detached jet that moves along the spine field lines above the null point.

The velocity pulses launched by the photosphere motions and granular power can launch the spicule-like small-scale plasma jets in the lower solar atmosphere (Murawski and Zaqarashvili, 2010; Malins and Erdélyi, 2007). However, in the active regions, the reconnection event and large energy deposition can generate the strong velocity pulses that launch such type of pulse-driven observed plasma blobs. Therefore, the reconnection-generated velocity pulse is found to be an efficient driver of the supersonic plasma blob. The energy release by a recurrent 3-D reconnection process via the separator dome below the magnetic null point, between the emerging flux and pre-existing field lines in the lower solar atmosphere, is found to be the driver of a radial velocity pulse outwards that accelerates this plasma blob in the solar atmosphere. The observed magnetic field and its extrapolation at the flare site mimic the formation of a 3D null point and the reconnection through the separator dome that are well established in

theory (Aschwanden, 2004). Our numerical modelling shows the formation of a supersonic plasma blob with a speed of $\sim 215 \text{ km s}^{-1}$ that is triggered due to the generation of a Gaussian velocity pulse at a height of 5 Mm from the photosphere where the low-lying quadrupolar loop system probably reconnects (cf., Figs 1,2,5). The pulse steepens into shock with the evolution of temperature gradient, and the low pressure behind it causing the uplift of cool low atmospheric plasma in the corona. The observation of multi-temperature plasma in the blob matches well with this evolution of the multi-temperature plasma in various parts of the simulated plasma blob, i.e., the cool confined material enveloped by a heated plasma. The observed supersonic blob powered by reconnection-generated velocity pulse may be very significant in fulfilling the coronal energy losses above an active region, if they occur repeatedly in the corona. This is the unique observational evidence of such high-speed energy packets which may occur under the particular magnetic field configuration in the flaring regions. If we assume the typical coronal electron density above active region loop-like field configuration $n_e = 1.0 \times 10^{10} \text{ cm}^{-3}$, the phase speed $V_{ph} = 215 \text{ km s}^{-1}$, and the non-thermal speed in form of unresolved mass motions in the coronal plasma as $V_{nt} = 40 \text{ km s}^{-1}$, then such MHD pulse-driven blobs may carry an energy flux of $E_f = 7.0 \times 10^6 \text{ ergs cm}^{-2} \text{ s}^{-1}$ to submit in the corona, if their origin is non-thermal as in this case. This energy transport may be very sufficient to contribute to re-balance the coronal losses above active regions.

In conclusions, these first observations provide important clues about the plasma dynamics driven by a velocity pulse, and its role in energy transport in the solar atmosphere. The rare multiwavelength observations of the blob propagation in the solar corona also provides the clues of steady reconnection process in the low atmosphere well before the flaring event. Further multi-wavelength observational studies will be required to shed more light on the transport of the mass and energy by such reconnection generated and pulse driven plasma eruptions.

Acknowledgements We acknowledge the remarks of the referee during review process of our manuscript. AKS thanks SP2RC, School of Mathematics and Statistics, The University of Sheffield for the support of collaborative visit, where the part of present research work has been carried out. AKS also acknowledges discussions with Boris Filippov, M. Opher, E. Verwichte, and to Shobhna Srivastava for her support and encouragement during the work. We also acknowledge MDI/SoHO and TRACE observations used in this study. We also thank Culgoora Solar Observatory at Narrabri, Australia to provide the H-alpha images. RE acknowledges M. K  ray for patient encouragement and is also grateful to NSF, Hungary (OTKA, Ref. No. K83133) for support received. The software used in this work was in part developed by the DOE-supported ASC/Alliance Center for Astrophysical Thermonuclear Flashes at the University of Chicago.

References

- Andries, J., van Doorselaere, T., Roberts, B., Verth, G., Verwichte, E., Erd  lyi, R.: 2009, Coronal Seismology by Means of Kink Oscillation Overtones. *Space Sci. Rev.* **149**, 3–29. doi:10.1007/s11214-009-9561-2.

- Archontis, V., Hood, A.W.: 2010, Flux emergence and coronal eruption. *Astron. Astrophys.* **514**, 56. doi:10.1051/0004-6361/200913502.
- Aschwanden, M.J.: 2004, *Physics of the Solar Corona. An Introduction*, Praxis Publishing Ltd, ???.
- Aschwanden, M.J.: 2009, The 3D Geometry, Motion, and Hydrodynamic Aspects of Oscillating Coronal Loops. *Space Sci. Rev.* **149**, 31–64. doi:10.1007/s11214-009-9505-x.
- Aschwanden, M.J., Fletcher, L., Schrijver, C.J., Alexander, D.: 1999, Coronal Loop Oscillations Observed with the Transition Region and Coronal Explorer. *Astrophys. J.* **520**, 880–894. doi:10.1086/307502.
- Ballai, I., Erdélyi, R., Pintér, B.: 2005, On the Nature of Coronal EIT Waves. *Astrophys. J.* **633**, 145–148. doi:10.1086/498447.
- Bárta, M., Karlický, M., Žemlička, R.: 2008, Plasmoid Dynamics in Flare Reconnection and the Frequency Drift of the Drifting Pulsating Structure. *Solar Phys.* **253**, 173–189. doi:10.1007/s11207-008-9217-5.
- Bárta, M., Karlický, M., Vršnak, B., Goossens, M.: 2007, MHD Waves and Shocks Generated during Magnetic Field Reconnection. *Central European Astrophysical Bulletin* **31**, 165.
- Benz, A.O.: 2008, Flare observations. *Living Reviews in Solar Physics* **5**(1). <http://www.livingreviews.org/lrsp-2008-1>.
- Botha, G.J.J., Arber, T.D., Srivastava, A.K.: 2012, Observational Signatures of the Coronal Kink Instability with Thermal Conduction. *Astrophys. J.* **745**, 53. doi:10.1088/0004-637X/745/1/53.
- Canou, A., Amari, T., Bommier, V., Schmieder, B., Aulanier, G., Li, H.: 2009, Evidence for a Pre-Eruptive Twisted Flux Rope Using the Themis Vector Magnetograph. *Astrophys. J.* **693**, 27–30. doi:10.1088/0004-637X/693/1/L27.
- Carlsson, M., Judge, P.G., Wilhelm, K.: 1997, SUMER Observations Confirm the Dynamic Nature of the Quiet Solar Outer Atmosphere: The Internetwork Chromosphere. *Astrophys. J.* **486**, 63. doi:10.1086/310836.
- Cirtain, J.W., Golub, L., Lundquist, L., van Ballegooijen, A., Savcheva, A., Shimojo, M., DeLuca, E., Tsuneta, S., Sakao, T., Reeves, K., Weber, M., Kano, R., Narukage, N., Shibasaki, K.: 2007, Evidence for Alfvén Waves in Solar X-ray Jets. *Science* **318**, 1580. doi:10.1126/science.1147050.
- Cooper, F.C., Nakariakov, V.M., Williams, D.R.: 2003, Short period fast waves in solar coronal loops. *Astron. Astrophys.* **409**, 325–330. doi:10.1051/0004-6361:20031071.
- Culhane, L., Harra, L.K., Baker, D., van Driel-Gesztelyi, L., Sun, J., Doschek, G.A., Brooks, D.H., Lundquist, L.L., Kamio, S., Young, P.R., Hansteen, V.H.: 2007, Hinode EUV Study of Jets in the Sun’s South Polar Corona. *Pub. Astron. Soc. Japan* **59**, 751.
- De Pontieu, B., Erdélyi, R.: 2006, The nature of moss and lower atmospheric seismology. *Royal Society of London Philosophical Transactions Series A* **364**, 383–394. doi:10.1098/rsta.2005.1704.
- De Pontieu, B., Erdélyi, R., James, S.P.: 2004, Solar chromospheric spicules from the leakage of photospheric oscillations and flows. *Nature* **430**, 536–539. doi:10.1038/nature02749.
- De Pontieu, B., McIntosh, S., Hansteen, V.H., Carlsson, M., Schrijver, C.J., Tarbell, T.D., Title, A.M., Shine, R.A., Suematsu, Y., Tsuneta, S., Katsukawa, Y., Ichimoto, K., Shimizu, T., Nagata, S.: 2007, A Tale of Two Spicules: The Impact of Spicules on the Magnetic Chromosphere. *Pub. Astron. Soc. Japan* **59**, 655.
- Erdélyi, R., Taroyan, Y.: 2008, Hinode EUV spectroscopic observations of coronal oscillations. *Astron. Astrophys.* **489**, 49–52. doi:10.1051/0004-6361:200810263.
- Erdélyi, R., Verth, G.: 2007, The effect of density stratification on the amplitude profile of transversal coronal loop oscillations. *Astron. Astrophys.* **462**, 743–751. doi:10.1051/0004-6361:20065693.
- Filippov, B., Golub, L., Koutchmy, S.: 2009, X-Ray Jet Dynamics in a Polar Coronal Hole Region. *Solar Phys.* **254**, 259–269. doi:10.1007/s11207-008-9305-6.
- Foullon, C., Verwichte, E., Nakariakov, V.M., Fletcher, L.: 2005, X-ray quasi-periodic pulsations in solar flares as magnetohydrodynamic oscillations. *Astron. Astrophys.* **440**, 59–62. doi:10.1051/0004-6361:200500169.
- Foullon, C., Verwichte, E., Nakariakov, V.M., Nykyri, K., Farrugia, C.J.: 2011, Magnetic Kelvin-Helmholtz Instability at the Sun. *Astrophys. J.* **729**, 8. doi:10.1088/2041-8205/729/1/L8.
- Innes, D.E., Inhester, B., Axford, W.I., Wilhelm, K.: 1997, Bi-directional plasma jets produced by magnetic reconnection on the Sun. *Nature* **386**, 811–813. doi:10.1038/386811a0.

- Katsukawa, Y., Berger, T.E., Ichimoto, K., Lites, B.W., Nagata, S., Shimizu, T., Shine, R.A., Suematsu, Y., Tarbell, T.D., Title, A.M., Tsuneta, S.: 2007, Small-Scale Jetlike Features in Penumbra Chromospheres. *Science* **318**, 1594. doi:10.1126/science.1146046.
- Kukhianidze, V., Zaqarashvili, T.V., Khutsishvili, E.: 2006, Observation of kink waves in solar spicules. *Astron. Astrophys.* **449**, 35–38. doi:10.1051/0004-6361/200600018.
- Kumar, M., Srivastava, A.K., Dwivedi, B.N.: 2011, Observation of intensity oscillations above X-ray bright points from the Hinode/XRT: signature of magnetohydrodynamic oscillations in the solar corona. *Mon. Not. Roy. Astron. Soc.* **415**, 1419–1425. doi:10.1111/j.1365-2966.2011.18792.x.
- Kumar, P., Srivastava, A.K., Somov, B., Manoharan, P., Erdelyi, R., Uddin, W.: 2010, Evidence of Solar Flare Triggering due to Loop-Loop Interaction Caused by Footpoint Shear Motion. *Astrophys. J.*, 110. doi:10.1007/s11207-010-9586-4.
- Kumar, P., Srivastava, A.K., Filippov, B., Uddin, W.: 2010, Multiwavelength Study of the M8.9/3B Solar Flare from AR NOAA 10960. *Solar Phys.*
- Kundu, M.R., Nindos, A., Vilmer, N., Klein, K., Shibata, K., Ohyama, M.: 2001, Metric Radio Emission Associated with X-Ray Plasmoid Ejections. *Astrophys. J.* **559**, 443–451. doi:10.1086/322301.
- Lee, D., Deane, A.E.: 2009, An unsplit staggered mesh scheme for multidimensional magnetohydrodynamics. *Journal of Computational Physics* **228**, 952–975. doi:10.1016/j.jcp.2008.08.026.
- Li, H., Schmieder, B., Song, M.T., Bommier, V.: 2007, Interaction of magnetic field systems leading to an X1.7 flare due to large-scale flux tube emergence. *Astron. Astrophys.* **475**, 1081–1091. doi:10.1051/0004-6361/20077500.
- Lin, J., Ko, Y., Sui, L., Raymond, J.C., Stenborg, G.A., Jiang, Y., Zhao, S., Mancuso, S.: 2005, Direct Observations of the Magnetic Reconnection Site of an Eruption on 2003 November 18. *Astrophys. J.* **622**, 1251–1264. doi:10.1086/428110.
- Liu, R., Alexander, D., Gilbert, H.R.: 2007, Kink-induced Catastrophe in a Coronal Eruption. *Astrophys. J.* **661**, 1260–1271. doi:10.1086/513269.
- Loureiro, N.F., Schekochihin, A.A., Cowley, S.C.: 2007, Instability of current sheets and formation of plasmoid chains. *Physics of Plasmas* **14**(10), 100703. doi:10.1063/1.2783986.
- Malins, C., Erdélyi, R.: 2007, Direct Propagation of Photospheric Acoustic p Modes into Nonmagnetic Solar Atmosphere. *Solar Phys.* **246**, 41–52. doi:10.1007/s11207-007-9073-8.
- Manoharan, P.K., Kundu, M.R.: 2003, Coronal Structure of a Flaring Region and Associated Coronal Mass Ejection. *Astrophys. J.* **592**, 597–606. doi:10.1086/375700.
- Manoharan, P.K., Kundu, M.R.: 2003, Coronal Structure of a Flaring Region and Associated Coronal Mass Ejection. *Astrophys. J.* **592**, 597–606. doi:10.1086/375700.
- Milligan, R.O., McAteer, R.T.J., Dennis, B.R., Young, C.A.: 2010, Evidence of a Plasmoid-Looptop Interaction and Magnetic Inflows During a Solar Flare/Coronal Mass Ejection Eruptive Event. *Astrophys. J.* **713**, 1292–1300. doi:10.1088/0004-637X/713/2/1292.
- Murawski, K., Zaqarashvili, T.V.: 2010, Numerical simulations of spicule formation in the solar atmosphere. *Astron. Astrophys.* **519**, 8. doi:10.1051/0004-6361/201014128.
- Murawski, K., Srivastava, A.K., Zaqarashvili, T.V.: 2011, Numerical simulations of solar macrospicules. *Astron. Astrophys.* **535**, 58. doi:10.1051/0004-6361/201117589.
- Nagashima, K., Isobe, H., Yokoyama, T., Ishii, T.T., Okamoto, T.J., Shibata, K.: 2007, Triggering Mechanism for the Filament Eruption on 2005 September 13 in NOAA Active Region 10808. *Astrophys. J.* **668**, 533–545. doi:10.1086/521139.
- Nakariakov, V.M., Arber, T.D., Ault, C.E., Katsiyannis, A.C., Williams, D.R., Keenan, F.P.: 2004, Time signatures of impulsively generated coronal fast wave trains. *Mon. Not. Roy. Astron. Soc.* **349**, 705–709. doi:10.1111/j.1365-2966.2004.07537.x.
- Nakariakov, V.M., Foullon, C., Verwichte, E., Young, N.P.: 2006, Quasi-periodic modulation of solar and stellar flaring emission by magnetohydrodynamic oscillations in a nearby loop. *Astron. Astrophys.* **452**, 343–346. doi:10.1051/0004-6361/20054608.
- Nishizuka, N., Shimizu, M., Nakamura, T., Otsuji, K., Okamoto, T.J., Katsukawa, Y., Shibata, K.: 2008, Giant Chromospheric Anemone Jet Observed with Hinode and Comparison with Magnetohydrodynamic Simulations: Evidence of Propagating Alfvén Waves and Magnetic Reconnection. *Astrophys. J.* **683**, 83–86. doi:10.1086/591445.
- Nishizuka, N., Takasaki, H., Asai, A., Shibata, K.: 2010, Multiple Plasmoid Ejections and Associated Hard X-ray Bursts in the 2000 November 24 Flare. *Astrophys. J.* **711**, 1062–1072. doi:10.1088/0004-637X/711/2/1062.

- Nisticò, G., Bothmer, V., Patsourakos, S., Zimbardo, G.: 2009, Characteristics of EUV Coronal Jets Observed with STEREO/SECCHI. *Solar Phys.* **259**, 87–108. doi:10.1007/s11207-009-9424-8.
- Ofman, L.: 2009, Progress, Challenges, and Perspectives of the 3D MHD Numerical Modeling of Oscillations in the Solar Corona. *Space Sci. Rev.* **149**, 153–174. doi:10.1007/s11214-009-9501-1.
- Pariat, E., Antiochos, S.K., DeVore, C.R.: 2009, A Model for Solar Polar Jets. *Astrophys. J.* **691**, 61–74. doi:10.1088/0004-637X/691/1/61.
- Patsourakos, S., Pariat, E., Vourlidas, A., Antiochos, S.K., Wuelser, J.P.: 2008, STEREO SECCHI Stereoscopic Observations Constraining the Initiation of Polar Coronal Jets. *Astrophys. J.* **680**, 73–76. doi:10.1086/589769.
- Petschek, H.E.: 1964, Magnetic Field Annihilation. *NASA Special Publication* **50**, 425.
- Riley, P., Lionello, R., Mikić, Z., Linker, J., Clark, E., Lin, J., Ko, Y.: 2007, “Bursty” Reconnection Following Solar Eruptions: MHD Simulations and Comparison with Observations. *Astrophys. J.* **655**, 591–597. doi:10.1086/509913.
- Roberts, B., Webb, A.R.: 1979, Vertical motions in an intense magnetic flux tube. III - On the slender flux tube approximation. *Solar Phys.* **64**, 77–92. doi:10.1007/BF00151117.
- Roberts, B., Edwin, P.M., Benz, A.O.: 1983, Fast pulsations in the solar corona. *Nature* **305**, 688–690. doi:10.1038/305688a0.
- Roussev, I., Galsgaard, K., Erdélyi, R., Doyle, J.G.: 2001, Modelling of explosive events in the solar transition region in a 2D environment. I. General reconnection jet dynamics. *Astron. Astrophys.* **370**, 298–310. doi:10.1051/0004-6361:20010207.
- Ruderman, M.S., Erdélyi, R.: 2009, Transverse Oscillations of Coronal Loops. *Space Sci. Rev.* **149**, 199–228. doi:10.1007/s11214-009-9535-4.
- Selwa, M., Ofman, L.: 2010, The Role of Active Region Topology in Excitation, Trapping, and Damping of Coronal Loop Oscillations. *Astrophys. J.* **714**, 170–177. doi:10.1088/0004-637X/714/1/170.
- Selwa, M., Ofman, L., Murawski, K.: 2007, Numerical Simulations of Slow Standing Waves in a Curved Solar Coronal Loop. *Astrophys. J.* **668**, 83–86. doi:10.1086/522602.
- Sheeley, N.R. Jr., Wang, Y.: 2002, Characteristics of Coronal Inflows. *Astrophys. J.* **579**, 874–887. doi:10.1086/342923.
- Srivastava, A.K., Dwivedi, B.N.: 2010, Observations from Hinode/EIS of intensity oscillations above a bright point: signature of the leakage of acoustic oscillations in the inner corona. *Mon. Not. Roy. Astron. Soc.* **405**, 2317–2326. doi:10.1111/j.1365-2966.2010.16651.x.
- Srivastava, A.K., Murawski, K.: 2011, Observations of a pulse-driven cool polar jet by SDO/AIA. *Astron. Astrophys.* **534**, 62. doi:10.1051/0004-6361/201117359.
- Srivastava, A.K., Murawski, K.: 2012, Observations of Post-flare Plasma Dynamics during an M1.0 Flare in AR11093 by the Solar Dynamics Observatory/Atmospheric Imaging Assembly. *Astrophys. J.* **744**, 173. doi:10.1088/0004-637X/744/2/173.
- Srivastava, A.K., Zaqarashvili, T.V., Kumar, P., Khodachenko, M.L.: 2010, Observation of Kink Instability During Small B5.0 Solar Flare on 2007 June 4. *Astrophys. J.*
- Taroyan, Y., Erdélyi, R.: 2009, Heating Diagnostics with MHD Waves. *Space Sci. Rev.* **149**, 229–254. doi:10.1007/s11214-009-9506-9.
- Taroyan, Y., Erdélyi, R., Wang, T.J., Bradshaw, S.J.: 2007, Forward Modeling of Hot Loop Oscillations Observed by SUMER and SXT. *Astrophys. J.* **659**, 173–176. doi:10.1086/517521.
- Terradas, J.: 2009, Excitation of Standing Kink Oscillations in Coronal Loops. *Space Sci. Rev.* **149**, 255–282. doi:10.1007/s11214-009-9560-3.
- Terradas, J., Andries, J., Goossens, M.: 2007, Coronal loop oscillations: energy considerations and initial value problem. *Astron. Astrophys.* **469**, 1135–1143. doi:10.1051/0004-6361:20077404.
- Vernazza, J.E., Avrett, E.H., Loeser, R.: 1981, Structure of the solar chromosphere. III - Models of the EUV brightness components of the quiet-sun. *Astrophys. J.* **45**, 635–725. doi:10.1086/190731.
- Veronig, A.M., Rybák, J., Gömöry, P., Berkebile-Stoiser, S., Temmer, M., Otruba, W., Vršnak, B., Pötzi, W., Baumgartner, D.: 2010, Multiwavelength Imaging and Spectroscopy of Chromospheric Evaporation in an M-class Solar Flare. *Astrophys. J.* **719**, 655–670. doi:10.1088/0004-637X/719/1/655.
- Wang, T., Solanki, S.K., Curdt, W., Innes, D.E., Dammasch, I.E.: 2002, Doppler Shift Oscillations of Hot Solar Coronal Plasma Seen by SUMER: A Signature of Loop Oscillations? *Astrophys. J.* **574**, 101–104. doi:10.1086/342189.

- Wang, Y., Xue, X., Shen, C., Ye, P., Wang, S., Zhang, J.: 2006, Impact of Major Coronal Mass Ejections on Geospace during 2005 September 7-13. *Astrophys. J.* **646**, 625–633. doi:10.1086/504676.
- Yokoyama, T., Akita, K., Morimoto, T., Inoue, K., Newmark, J.: 2001, Clear Evidence of Reconnection Inflow of a Solar Flare. *Astrophys. J.* **546**, 69–72. doi:10.1086/318053.
- Zaqarashvili, T.V., Kukhianidze, V., Khodachenko, M.L.: 2010, Propagation of a sausage soliton in the solar lower atmosphere observed by Hinode/SOT. *Mon. Not. Roy. Astron. Soc.* **404**, 74–78. doi:10.1111/j.1745-3933.2010.00838.x.